Chapter 4

TUMOR XENOGRAFT UPTAKE OF A PYRROLE–IMIDAZOLE
(PY-IM) POLYAMIDE VARIES AS A FUNCTION OF CELL LINE GRAFTED

The text of this chapter was taken in part from a manuscript co-authored with Jevgenij A. Raskatov and Peter B. Dervan.

(Raskatov JA, Szablowski JO, Dervan PB, "Tumor Xenograft Uptake of a Py Im Polyamide Varies as a Function of Cell Line Grafted", J. Med Chem. 57(20):8471-6 (2013))

Abstract

Subcutaneous xenografts represent a popular approach to evaluate efficacy of prospective molecular therapeutics *in vivo*. In the present study, the C-14 labeled radioactive Py-Im polyamide 1, targeted to the 5'-WGWWCW-3' DNA sequence, was evaluated with regard to its uptake properties in subcutaneous xenografts, derived from the human tumor cell lines LNCaP (prostate), A549 (lung), and U251 (brain), respectively. Significant variation in compound tumor concentrations was seen in xenografts derived from these three cell lines. Influence of cell line grafted on systemic polyamide elimination was established. With A549, a marked variation in localization of 1 was determined between matrigel-negative and -positive xenografts. An extensive tissue distribution analysis of 1 in wild-type animals was conducted, enabling the comparison between the xenografts and the corresponding host organs of origin.

Introduction

Cancer represents a major worldwide health problem, with nearly 1.6 million new cases estimated to occur in 2014 in the US alone.[1] The past forty years of research and development of therapeutics has brought improved patients' survival[2], however, malignant neoplasias remain the second most common cause of death in the US, accounting for over 20 % of all deaths.[3] Consequentially, major efforts are being put into the development of novel therapeutic approaches.[4] Treatment strategies of various classes are currently available in the clinic. Classical approaches comprise surgery, chemotherapy, radiation therapy and immunotherapy, with the method of choice depending on tumor type and progression stage.[5] Cancer chemotherapy has recently seen important conceptual advances, such as tumor-specific tissue targeting,[6] prodrug modifications,[7] and development of small molecule inhibitors of aberrant signaling nodes in cancer.[8] A significant drawback of mole-cules targeted to tumor-specific features is the introduction of evolutionary pressure upon the cancer cells, which often results in the emergence of resistant clones.[9] Broadly cytotoxic chemotherapeutics (*e.g., cis*-platin or doxorubicin), on the other hand, commonly exhibit severe side-effects, such as cardio-,[10] and neurotoxicity,[11] as well as neutropenia.[12]

Py-Im polyamides are a modular class of DNA-binding small molecules, capable of binding defined sequences with affinities and specificities comparable to those of DNA-binding proteins.[13] They are cell-permeable scaffolds,[14] and have been shown to displace various transcription factors from cognate binding sites[15], leading to altered gene expression profiles. Inhibition of RNA pol II elongation was observed, accompanied by degradation of the large RNA pol II subunit and induction of the p53 stress response,

without concomitant DNA damage.[16] Most recently, our laboratory has transitioned to

in vivo experimentation, demonstrating bioavailability,[17] and efficacy of varying Py-Im

polyamides in tumor xenografts models in mouse.[16,18] Antitumor effects with limited

systemic toxicity were observed with the subcutaneous LNCaP prostate cancer model.[16]

Our recent C-14 based quantitation study established significant enrichment of a Py-Im

polyamide in the LNCaP tumor xenograft tissue over lung and kidney.[19] The present

investigation evaluates the biodistribution of the C-14 radioactively labeled Py-Im

polyamide **1** (Fig. 4. 1A) in a range of tumor xenografts, addresses the influence of

xenografted cell line on systemic polyamide elimination, and provides an extended

biodistribution profile of the molecule.

Results

C-14 radioactively labeled Py-Im polyamide 1 exhibits differential uptake between tumor xenografts of varying cellular origin. Initial experiments compared the accumulation of compound **1** in LNCaP and A549 subcutaneous tumor xenografts (Fig. 4.1A). In order to minimize the injection-associated experimental error, both tumors were grafted on the opposing flanks of the same host animal, following the schedule displayed in Fig. 4.2. A mean compound concentration of 1.04 mg/kg (0.74 μM) was measured for the LNCaP xenograft tissue, comparable with liver-associated levels of 1.12 mg/kg (Fig. 4.1B). Strikingly, A549 tumors were found to uptake substantially lower amounts of polyamide **1** (average of 0.23 mg/kg), closely resembling the values obtained for the kidney (0.27 mg/kg), and approximately two-fold higher than lung tissue (0.15 mg/kg). Comparisons with the corresponding single-xenograft versions of the experiment were conducted for both tumor types (Fig. 4.1C). The LNCaP single tumor experiment revealed a mildly elevated concentration with respect to the double xenograft counterpart (42 %, p < 0.05),[19] whereas the values obtained for A549 were not distinguishable between the two experiment types. Overall, Py-Im polyamide **1** localized to LNCaP (prostate) tumors at concentrations five to seven-fold higher than those measured with A549 (lung).

To gain deeper understanding of the phenomenon, immunohistochemical analyses were conducted, assaying for tumor-associated microvessels (Figures 3 and 4). Microvessel densities were indistinguishable between the two tumor types. However, LNCaP xenografts were hemorrhagic and exhibited vascular spaces with extravasated red blood cells at the microscopic level, which were absent with A549. In order to broaden the scope
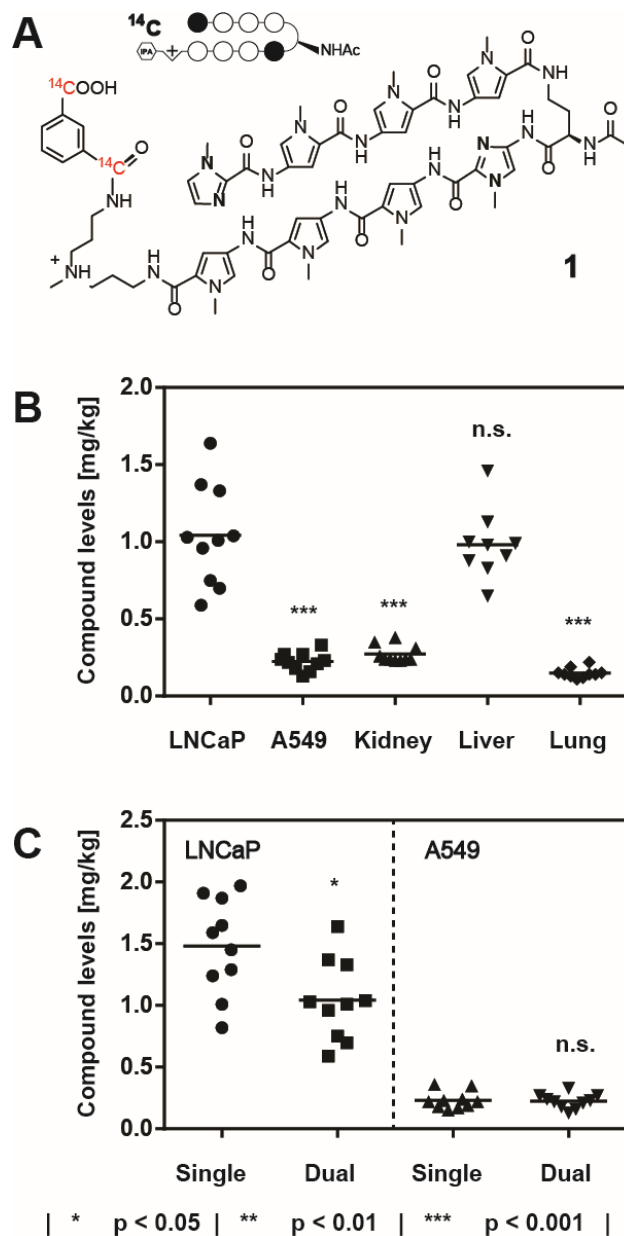
Fig. 4.1. A) The C-14 radiolabeled Py-Im polyamide **1**, targeted to the DNA sequence 5'-WGWWCW-3'. B) Compound levels of **1** in LNCaP and A549 tumor xenografts, compared against major host organs (kidney, liver, lung). Statistical comparison performed against the LNCaP tumor concentration of **1**. C) Calibration of the dual xenograft experiment against the respective single-tumor versions. All injections were performed intraperitoneally at 20 nmol per animal (NSG male mouse, N=10) and tissues harvested 24 hours following administration. Each datapoint represents an individual organ / tumor analyzed.
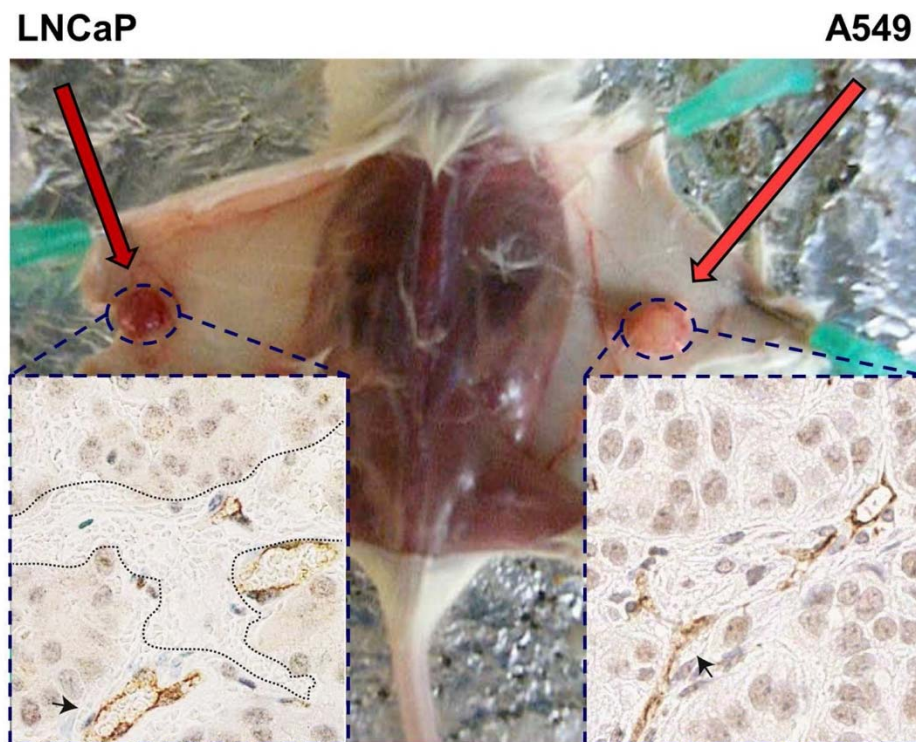
Fig. 4.2. Engraftment and polyamide administration schedules for the double flank experiment and the single flank versions.

of the investigation, the U251 (brain) cell line was additionally evaluated in the xenograft setting with regard to uptake of 1 (Fig. 4.5). A mean value of 0.65 mg/kg (0.47 μM) was measured. The U251-associated xenograft uptake profile was found to be distinct from both LNCaP and A549-derived tissues, which were 2.3-fold higher and 2.8-fold lower, respectively.

None of the tumor-associated levels of Py-Im polyamide **1**, discussed above, exhibited a correlation with tumor size over the window analyzed (Fig. 4.6A-D,F).

Fig. 4.3. A representative NSG male mouse that was grafted with LNCaP (2.5×10^6 in 1:1 media / matrigel) and A549 (2.5×10^6 in media), following schedule outlined in (A). Representative histological slices (CD31 stain) are displayed in the inset graphics. LNCaP tumor displays poorly defined vascular spaces with extravasated red blood cells (indicated with the dotted line), absent with A549. Arrows highlight some blood vessels.

Host organ levels of Py-Im polyamide 1 as a function of the subcutaneously grafted cell line. The major host organs kidney, liver, and lung were interrogated with regard to concentrations of **1** for all xenograft experiments, and benchmarked against the naïve background control (Fig. 4.7). Kidney concentrations spanned a range from 0.22 mg /kg (naïve control and A549 xenograft animals) to 0.27 mg/kg (double xenograft experiment).
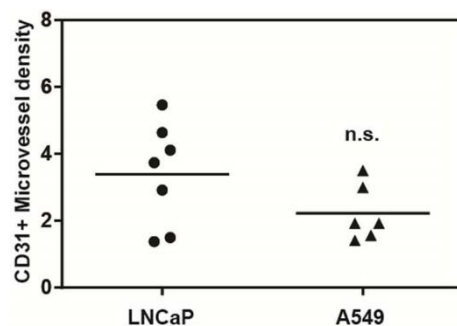
Fig. 4.4. Microvessel density quantitated for LNCaP and A549 tumor sections, respectively.
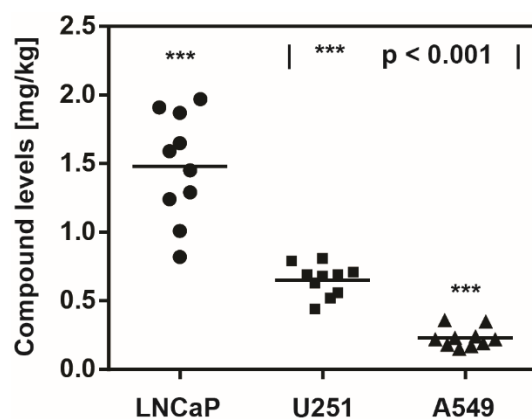

Fig. 4.5. Tumor levels of Py-Im polyamide **1** as a function of cell line engrafted. All injections were performed intraperitoneally at 20 nmol per animal (NSG male mouse, N=10) and tissues harvested 24 hours following administration. Each datapoint represents an individual tumor analyzed. Statistical comparison was performed against the U251 tumor concentration of **1**.

Lung tissue showed similar variance in concentration of **1** as a function of xenografted cell line (0.12 to 0.15 mg/kg). A more significant difference was noted for the liver-associated compound levels. Whereas naïve reference animals were indistinguishable from U251- or A549-xenograft bearers, grafting of the LNCaP cell line resulted in liver values that were about two-fold higher (1.04 mg/kg vs 0.57 mg/kg; $p < 0.001$).

Matrigel affects uptake of Py-Im polyamide 1 into A549 xenografts. We chose to

evaluate the influence of matrigel on uptake of **1** for xenografts derived from the A549 cell

line. Systematic analysis of tumor polyamide concentration as a function of size revealed

that larger tumors accumulated substantially higher quantities of compound **1** when

matrigel was employed during engraftment (Fig. 4.6F). This was in striking contrast with

the observations made for the same cell line grafted without matrigel (Fig. 4.6A,C).
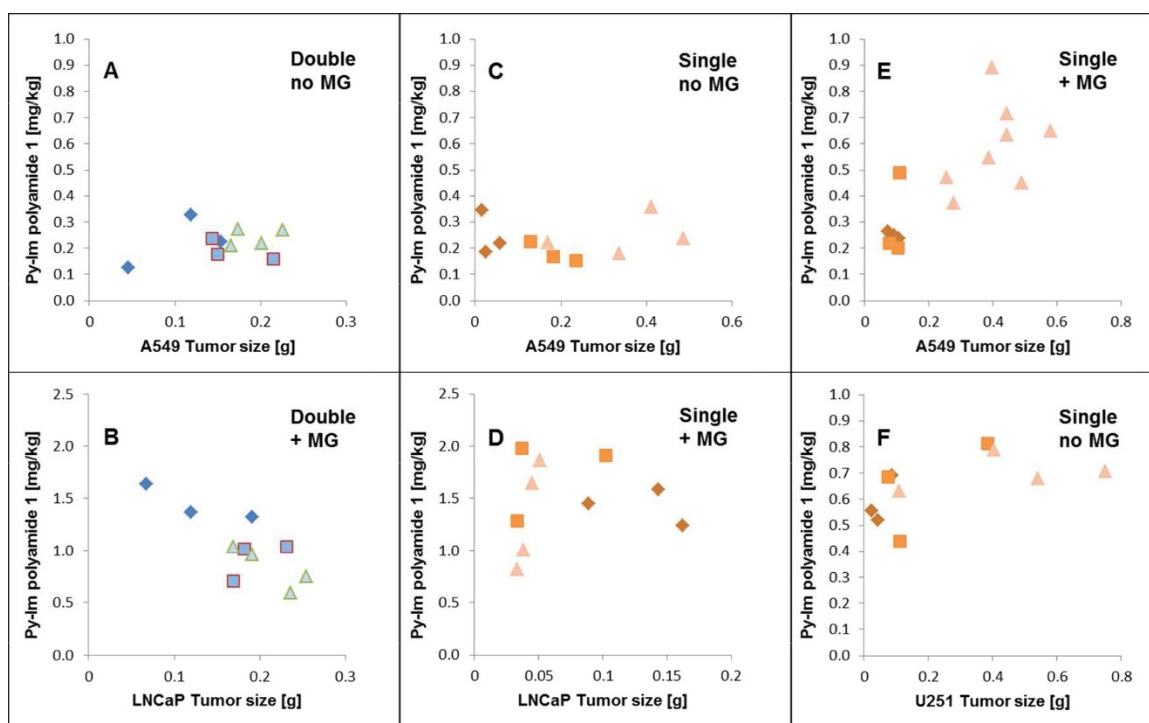

Fig. 4.6. Tumor concentration of Py-Im polyamide **1** as a function of size. MG denotes matrigel; double / single indicates whether the animals was grafted twice or once, respectively (only relevant with A549 and LNCaP). Post-engraftment time is coded by diamonds (4 weeks with LNCaP, 3 weeks with A549 or U251), squares (5 weeks with LNCaP, 4 weeks with A549 or U251), and triangles (6 weeks with LNCaP, 5 weeks with A549 or U251).
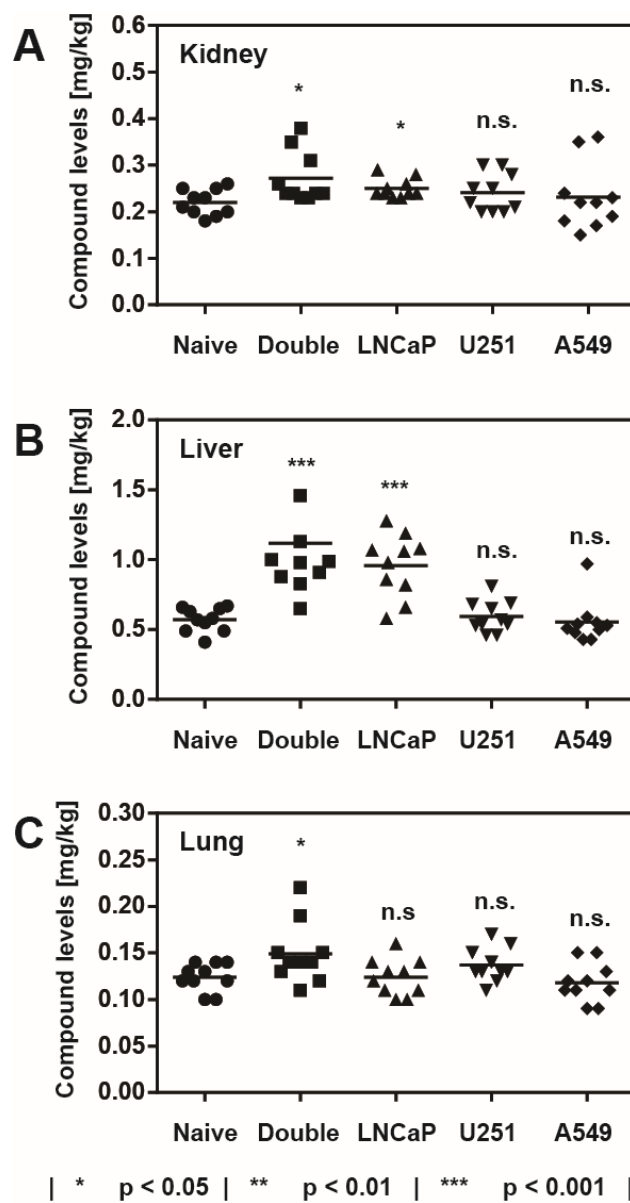
Fig. 4.7. Concentrations of polyamide **1** in the host organs kidney (A), liver (B), and lung (C) as a function of cell line engrafted. Naïve indicates reference host animals devoid of tumor graft. All injections were performed intraperitoneally at 20 nmol per animal (NSG male mouse, N=10) and tissues harvested 24 hours following administration. Each datapoint represents an individual organ analyzed.

Plotting of tumor-associated levels of **1** as a function of post-engraftment time revealed a clear trend (Fig. 4.8). Three or four weeks past engraftment, there was no statistically significant difference measurable between the A549 xenografts produced with or without matrigel, with an averaged concentration of 0.23 mg/kg (0.16 µM). Five weeks past engraftment, however, a divergence became apparent. Whereas matrigel-negative tumors showed levels of compound **1** indistinguishable from earlier timepoints (0.25mg/kg), a marked increase was noted for the matrigel-positive xenografts. A mean concentration of 0.59 mg/kg was measured ($p < 0.001$), with the highest value amounting to 0.89 mg/kg, therewith reaching values comparable to those obtained for LNCaP tumors (cf. Figures 1 and 5).

Extended tissue distribution analysis of 1 in wild-type mice. In order to obtain a more complete picture of biodistribution of Py-Im polyamide **1**, a comprehensive tissue analysis
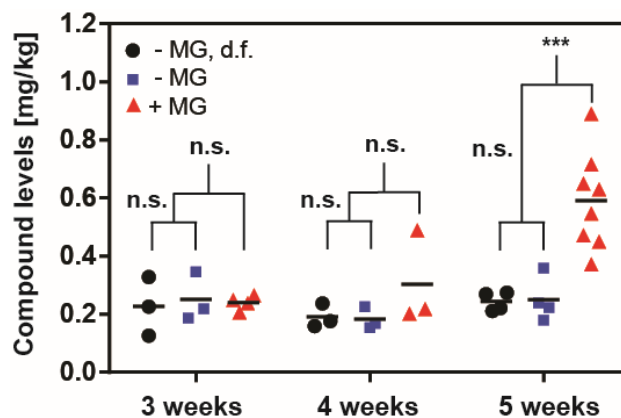

Fig. 4.8. A549 Tumor levels of Py-Im polyamide **1** as a function of time (3-5 weeks), presence of the LNCaP tumor on the opposite flank (denoted as d.f.), and matrigel used to engraft (+/- MG). All injections were performed intraperitoneally at 20 nmol per animal (NSG male mouse) and tumors harvested 24 hours following administration. Each datapoint represents an individual tumor analyzed. | *** $p < 0.001$ |

following administration of **1** was conducted in the balb/c mouse strain. Blood, bone marrow (BM), brain, fat tissue, intestinal tissue, heart, kidney, liver, lung, muscle, pancreas, prostate, and spleen were interrogated independently (Fig. 4.9). Because the balb/c male mouse of comparable age possesses a body weight that is reduced by some 25% with regard to its NSG counterpart, compound **1** was administered at 15 nmol per animal here, as opposed to 20 nmol per animal employed with NSG mice.

The majority of tissues exhibited concentrations of **1** below 0.1 mg/kg, with the brain not showing any significant evidence of polyamide uptake. Kidney and liver were found to contain comparable compound levels to those determined for the NSG strain (0.23 mg/kg vs 0.22 mg/kg and 0.57 mg/kg vs 0.49 mg/kg for kidney and liver, respectively). Interestingly, bone marrow concentration of **1** amounted to 0.24 mg/kg, therewith being over 10-fold higher than blood. The spleen exhibited a concentration of **1** of 0.32 mg/kg, whereas the pancreas contained compound **1** at 0.15 mg/kg. The majority of organs contained the Py-Im polyamide **1** at concentrations that were significantly lower than those determined for any of the tumor xenografts examined above.
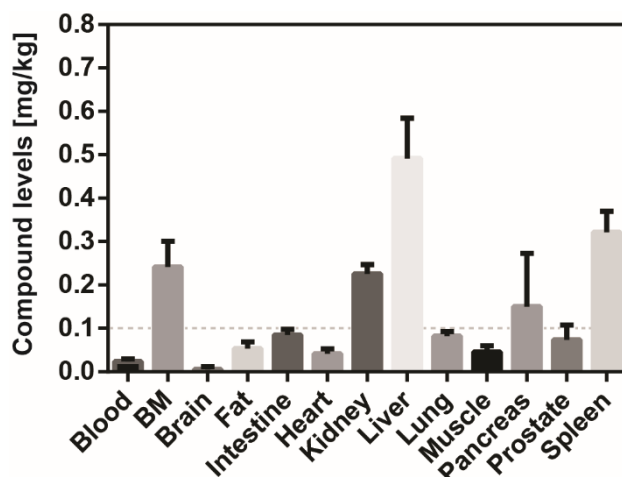
Fig. 4.9. Extended tissue distribution analysis of Py-Im polyamide **1** in wild-type mice. Injections were performed intraperitoneally at 15 nmol per animal (balb/c male mouse) and organs harvested 24 hours following administration. Error bars represent standard deviations (N = 5). BM denotes bone marrow. Dashed line indicates the 0.1 mg/kg threshold.

Discussion

The xenograft approach is a popular method to interrogate a prospective antitumor agent *in vivo*.[20] It can be subdivided into two main categories, namely subcutaneous (ectopic) and orthotopic xenografts. Orthotopic inoculation is considered to recapitulate the tumor setting more closely than the subcutaneous approach, because cancer cells are grafted into the host organ of tumor origin. With the exception of lung and blood cancer, for which orthotopic xenografts are readily achievable by tail vein injection, the approach is experimentally demanding, and requires sophisticated survival surgery. Genetically engineered animal tumor models represent an attracttive alternative to xenograft experimentation, since they tend to recapitulate certain aspects of disease progression, such as tumor vascularization, tumor-stroma interactions, and metastasis formation, more accurately.[21] They furthermore allow for conducting experiments in immunecompetent

animals. The studies are, however, elaborate to perform, requiring extended experimentation time frames and large animal group sizes. Furthermore, xenografts allow the assessment of efficacy against human cancer cell lines and primary cells, whereas genetically engineered animal models are limited to neoplasias of the species employed. Given the above, subcutaneous xenografts remain an attractive method to generate initial estimates of efficacy for molecules of interest.[22]

The present study was initiated to rationalize the apparent discrepancy between cell culture results and the corresponding xenograft experiments that we observed in preceding investigations.[16b,18a] Specifically, *in vitro* cytotoxicity evaluation for the non-radioactive analogue of **1** revealed A549 and LNCaP to possess comparable sensitivities towards polyamide treatment (IC_{50} values of 1.5 ± 0.2 μM and 2.1 ± 0.3 μM,[16b] respectively). This contrasted with the outcome of our *in vivo* investigations, with LNCaP xenografts exhibiting tumor burden reduction in response to treatment with **1** in the xenograft setting,[16b] while related studies with the A549 cell line were unsuccessful.[18a] The present investigation demonstrates this unanticipated result to be rooted, at least in part, in the pronounced difference in polyamide uptake between the two xenograft types, LNCaP tumors accumulating the compound at five- to seven-fold higher levels than their A549 counterparts (Fig. 4.1) in both the double-flank experiment and the single xenograft experiments with A549 and LNCaP.[19] Additional discrepancy may stem from the difference in the time frame employed for *in vitro* cytotoxicity measurement (3 days) and *in vivo* antitumor evaluation (at least 7 days), and the fact that the polyamide concentration is kept constant over the course of the experiment *in vitro*, but not *in vivo*.[19]

Comparison with U251 xenografts revealed an uptake profile that was distinct from both LNCaP- and A549-derived tumors (Fig. 4.2). This leads to the important realization that neither LNCaP nor A549 could be considered an outlier. Each cell line examined yielded tumors with characteristic uptake features, which, while clearly dependent on the cell line grafted, could not have been predicted from *in vitro* experiments. The U251-derived xenografts exhibited higher microvessel densities than both A549 and LNCaP tumors, without, however, possessing the vascular spaces characteristic of LNCaP.[23] This likely gave rise to distinct characteristics of U251 tumors.

It was surprising to find that liver accumulation of **1** was dependent on the cell line grafted. Whereas the grafting of A549 or U251 cells showed no influence, the presence of LNCaP-derived tumors resulted in levels that were elevated by about twofold (Fig. 4.3). This was possibly due to the increased leakiness of the tumor vasculature in LNCaP xenografts, as compared with A549 (Fig. 4.SI 2), and U251.[23] Matrigel-positive xenografts did not result in increased liver compound values as compared to their matrigel-negative counterparts (0.65 mg/kg *vs* 0.55 mg/kg, p = 0.17). It is possible that the leaky LNCaP tumor vasculature creates liver stress, which in turn could result in impeded clearance of Py-Im polyamide **1**. This phenomenon is likely to operate with other types of small molecule therapeutics, although the magnitude of the effect will be dependent on specifics, which could lead to alternative clearance mechanisms.

The influence of matrigel on uptake of **1** by A549 xenografts was of interest due to the common use of matrigel to facilitate engraftment of tumor cells *in vivo*.[24] An effect indeed became manifest, albeit only at the most advanced post-engraftment timepoints (Fig. 4.4 and Fig. 4.SI 4E). It appears likely that the A549 tumor architecture diverges at advanced

time points, as a function of matrigel. Supporting this, slightly higher weights were noticed in the matrigel-positive group than in the matrigel-negative control at the point of divergence (average of 409 mg *vs* 271 mg; p < 0.05). Influence of matrigel employment on tumor proliferation, vascularization and metastasis have been previously documented.[24] The xenograft host-tumor interface being artificial *a priori*, it is unclear, whether the matrigel-positive or -negative tumors give rise to more accurate models.

Comparisons of uptake between tumors and the corresponding healthy host tissues were of interest, in order to probe for potential enrichment in cancer lesions. The LNCaP xenografts exhibited concentrations ranging from 0.5 mg/kg to 2.0 mg/kg, thus being an order of magnitude higher than what was determined for mouse prostate, which possessed an averaged value below 0.1 mg/kg. It is therefore possible that the compound quantities measured in LNCaP subcutaneous xenografts provide optimistic estimates. However, tumor formation does perturb organ integrity, and it therefore appears likely that diseased prostate tissue should exhibit values different from the healthy organ in both the orthotopic and the genetically induced disease model setting. It should furthermore be noted that LNCaP was derived from a metastatic lymph node lesion, which, although having originated from a prostate tumor, likely possessed a distinct architecture. Tumors derived from the A549 cell line (non-small lung carcinoma) can be compared with lung tissue concentrations of **1**. With the exception of the elevated values that were determined in matrigel-positive tumors at extended time points, they averaged at approximately 0.2 mg/kg, whereas healthy lung tissue exhibited concentrations of **1** around 0.1 mg/kg. Whether this is a coincidence or indeed evidence that A549 xenografts mimic the lung tissue setting more adequately remains unclear. Lung colonization experiments may be

useful to shed further light onto this question in future studies. U251 is a glioblastoma-derived cell line, and the healthy organ of origin is the brain. The corresponding comparison between tumor and tissue of origin lacks substance, since the subcutaneous xenograft cannot be expected to recapitulate the blood brain barrier. Overall, and keeping the above-mentioned caveats in mind, tumors generally accumulated higher amounts of compound **1** than the corresponding healthy tissues of origin.

Conclusions

The present study identified a marked difference in xenograft uptake levels of Py-Im polyamide **1** in the three cell lines tested. LNCaP-derived tumors exhibited a mean concentration of the polyamide that was over fivefold higher that the corresponding A549-associated value. Compound **1** was found to localize to U251 xenografts at a concentration that was substantially lower than what was found for LNCaP, but significantly higher than A549. This demonstrates the necessity of examining uptake into tumor xenografts on a case by case basis in order to rationalize outcomes of antitumor studies and to identify viable cell lines for future xenograft experiments. Unexpectedly, elimination of **1** from the liver was impaired in LNCaP xenograft-bearing animals. Matrigel was found to influence uptake of **1**, resulting in a twofold elevation at longer post-engraftment time points with A549-derived tumors. Comparison with the corresponding healthy tissues revealed that higher concentrations of **1** were associated with xenografts, with animal prostate tissue exhibiting order of magnitude lower values than those measured with LNCaP tumors.

Experimental Section

Polyamide Synthesis and Characterization. The synthesis of polyamide **1** has been previously reported.[19] The compound was confirmed by analytical HPLC to possess a purity of >99%, and co-eluted with its non-radioactive analog. Polyamide **1** was quantitated employing liquid scintillation with the activity constants of 55 mCi/mmol, which was provided by the vendor (ARC). Quench correction was conducted against a standard curve that was reported by our laboratory in a preceding account.[19]

Cell Culture Maintenance and Xenograft Establishment. The cell lines A549, LNCaP and U251 were obtained from ATCC and cultured following provider's recommendations, and not exceeding passage number 25. Cells were only employed for xenograft experimentation where a viability of 95 % or higher was recorded (trypan blue stain). Nod-SCID-Gamma (NSG) male mice were purchased at eight weeks of age from JAX and housed in an immunocompromised facility (level A) in accordance with IACUC regulations. They were taken forward for experiments after an acclimatization period of at least three days. All engraftments were conducted subcutaneously with 2.5 M cells per inoculation in 200 μL vehicle (either media or 1:1 mixture with matrigel). Animals were monitored weekly for signs of pain and distress. Male balb/c mice were obtained from JAX and housed in a level B animal facility.

Administration of polyamide 1 and tissue harvest. Compound **1** was quantitated by liquid scintillation counting prior to injection and administered intraperitoneally at either 20 nmol (NSG) or 15 nmol (balb/c) per animal in a fume hood dedicated exclusively to C-14 *in vivo* radioexperimentation. Animals were housed in disposable cages and euthanized by CO_2 asphyxiation. Disposable cages were destroyed at the end of the experiment.

Tissues were harvested, placed into scintillation vials, and solubilized at +65 °C for at least 12 hours, employing the proprietary dissolution agent SOLVABLE (Perkin-Elmer). The resultant solutions were decolorized with 2 x 200 μL hydrogen peroxide (30 %, Sigma Aldrich) at ambient temperature for at least 2 hours, followed by heating to +65 °C for 30 min. Samples were treated with 10 mL of the scintillation cocktail HIONIC-FLUOR (Perkin-Elmer), vortexed and the amounts of C-14 quantitated by liquid scintillation counting at the Beckman Coulter LS6500 Multi-Purpose Scintillation Counter. All reported values have been quench-corrected and normalized against organ weight. Bone marrow weights were calculated as the difference between the femur and tibia bones subjected to tissue solubilization, and the insoluble residue, which was isolated subsequent to C-14 quantitation. In order to obtain dry bone residues, the scintillation fluid was decanted, the solids triturated (twice with ethanol, then three times with MeOH), and dried at +65 °C overnight.

Acknowledgements

References

(1)Siegel, R.; Ma, J.; Zou, Z.; Jemal, A. Cancer statistics, 2014. *CA - Cancer J. Clin.* **2014**, *64*, 9-29.

(2)Ries, L. A. G. et al. SEER cancer statistics review, 1975-2005. *U.S. National Institutes of Health, National Cancer Institute,* **2008**.

(3)Hoyert, D. L.; Xu, J. Deaths: Preliminary Data for 2011. *Natl. Vital Stat. Rep.* **2012**, *61*, 1-52.

(4)Patel, J. D. et al. Clinical Cancer Advances 2013: Annual Report on Progress Against Cancer From the American Society of Clinical Oncology. *J. Clin. Oncol.* **2014**, *32*, 129-160.

(5)Huitink, J. M.; Teoh, W. H. L. Current cancer therapies – A guide for perioperative physicians. *Best Pract. Res. Cl. An.* **2013**, *27*, 481-492.

(6)Peer, D.; Karp, J. M.; Hong, S.; FaroKhzad, O. C.; Margalit, R.; Langer, R. Nanocarriers as an emerging platform for cancer therapy. *Nat. Nanotechnol.* **2007**, *2*, 751-760.

(7)Denny, W. A. Prodrug strategies in cancer therapy. *Eur. J. Med. Chem.* **2001**, *36*, 577-595.

(8)a) Druker, B. J. et al. Efficacy and safety of a specific inhibitor of the BCR-ABL tyrosine kinase in chronic myeloid leukemia. *N. Engl. J. Med.* **2001**, *344*, 1031-1037; b)

Baselga, J.; Arteaga, C. L. Critical update and emerging trends in epidermal growth factor receptor targeting in cancer. *J. Clin. Oncol.* **2005**, *23*, 2445-2459.

(9) Tsuruo, T.; Naito, M.; Tomida, A.; Fujita, N.; Mashima, T.; Sakamoto, H.; Haga, N. Molecular targeting therapy of cancer: drug resistance, apoptosis and survival signal. *Cancer Sci.* **2003**, *94*, 15-21.

(10) Pai, V. B.; Nahata, M. C. Cardiotoxicity of chemotherapeutic agents - Incidence, treatment and prevention. *Drug Saf.* **2000**, *22*, 263-302.

(11) Verstappen, C. C. P.; Heimans, J. J.; Hoekman, K.; Postma, T. J. Neurotoxic complications of chemotherapy in patients with cancer - Clinical signs and optimal management. *Drugs* **2003**, *63*, 1549-1563.

(12) Aapro, M. S. et al. EORTC guidelines for the use of granulocyte-colony stimulating factor to reduce the incidence of chemotherapy-induced febrile neutropenia in adult patients with lymphomas and solid tumours. *Eur. J. Cancer* **2006**, *42*, 2433-2453.

(13) a) Dervan, P. B.; Edelson, B. S. Recognition of the DNA minor groove by pyrrole-imidazole polyamides. *Curr. Opin. Struct. Biol.* **2003**, *13*, 284-299; b) Hsu, C. F. et al. Completion of a programmable DNA-binding small molecule library. *Tetrahedron* **2007**, *63*, 6146-6151; c) Kielkopf, C. L.; White, S.; Szewczyk, J. W.; Turner, J. M.; Baird, E. E.; Dervan, P. B.; Rees, D. C. A structural basis for recognition of A.T and T.A base pairs in the minor groove of B-DNA. *Science* **1998**, *282*, 111-115; d) White, S.; Szewczyk, J. W.; Turner, J. M.; Baird, E. E.; Dervan, P. B. Recognition of the four Watson-Crick base pairs in the DNA minor groove by synthetic ligands. *Nature* **1998**, *391*, 468-471.

(14) Edelson, B. S.; Best, T. P.; Olenyuk, B.; Nickols, N. G.; Doss, R. M.; Foister, S.; Heckel, A.; Dervan, P. B. Influence of structural variation on nuclear localization of DNA-binding polyamide-fluorophore conjugates. *Nucl. Acids Res.* **2004**, *32*, 2802-2818.

(15) a) Nickols, N. G.; Jacobs, C. S.; Farkas, M. E.; Dervan, P. B. Modulating hypoxia-inducible transcription by disrupting the HIF-1-DNA interface. *ACS Chem. Biol.* **2007**, *2*, 561-571; b) Nickols, N. G.; Dervan, P. B. Suppression of androgen receptor-mediated gene expression by a sequence-specific DNA-binding polyamide. *Proc. Natl. Acad. Sci. USA* **2007**, *104*, 10418-10423; c) Muzikar, K. A.; Nickols, N. G.; Dervan, P. B. Repression of DNA-binding dependent glucocorticoid receptor-mediated gene expression. *Proc. Natl. Acad. Sci. USA* **2009**, *106*, 16598-16603; d) Raskatov, J. A.; Meier, J. L.; Puckett, J. W.; Yang, F. T.; Ramakrishnan, P.; Dervan, P. B. Modulation of NF-κB-Dependent Gene Transcription Using Programmable DNA Minor Groove Binders. *Proc. Natl. Acad. Sci. USA* **2012**, *109*, 1023-1028.

(16) a) Yang, F.; Nickols, N. G.; Li, B. C.; Marinov, G. K.; Said, J. W.; Dervan, P. B. Antitumor activity of a pyrrole-imidazole polyamide. *Proc. Natl. Acad. Sci. U. S. A.* **2013**, *110*, 1863-1868; b) Yang, F.; Nickols, N. G.; Li, B. C.; Szablowski, J. O.; Hamilton, S. R.; Meier, J. L.; Wang, C.-M.; Dervan, P. B. Animal toxicity of hairpin pyrrole-imidazole polyamides varies with the turn unit. *J. Med. Chem.* **2013**, *56*, 7449-7457.

(17) a) Raskatov, J. A.; Hargrove, A. E.; So, A. Y.; Dervan, P. B. Pharmacokinetics of Py-Im Polyamides Depend on Architecture: Cyclic versus Linear. *J. Am. Chem. Soc.* **2012**, *134*, 7995-7999; b) Synold, T. W.; Xi, B. X.; Wu, J.; Yen, Y.; Li, B. C.; Yang, F.; Phillips,

J. W.; Nickols, N. G.; Dervan, P. B. Single-dose pharmacokinetic and toxicity analysis of pyrrole-imidazole polyamides in mice. *Cancer Chemother. Pharmacol.* **2012**, *70*, 617-625.

(18)a) Raskatov, J. A.; Nickols, N. G.; Hargrove, A. E.; Marinov, G. K.; Wold, B.; Dervan, P. B. Gene expression changes in a tumor xenograft by a pyrrole-imidazole polyamide. *Proc. Natl. Acad. Sci. U. S. A.* **2012**, *109*, 16041-16045; b) Nickols, N. G.; Szablowski, J. O.; Hargrove, A. E.; Li, B. C.; Raskatov, J. A.; Dervan, P. B. Activity of a Py-Im Polyamide Targeted to the Estrogen Response Element. *Mol. Cancer Ther.* **2013**, *12*, 675-684.

(19) Raskatov, J. A.; Puckett, J. W.; Dervan, P. B. A C-14 labeled Py–Im polyamide localizes to a subcutaneous prostate cancer tumor. *Bioorg. Med. Chem.*, http://dx.doi.org/10.1016/j.bmc.2014.1004.1010.

(20)Kerbel, R. S. Human Tumor Xenografts as Predictive Preclinical Models for Anticancer Drug Activity in Humans: Better than Commonly Perceived—But They Can Be Improved. *Cancer Biol. Ther.* **2003**, *2*, 133 - 138.

(21)a) Frese, K. K.; Tuveson, D. A. Maximizing mouse cancer models. *Nat. Rev. Cancer* **2007**, *7*, 645-658; b) Becher, O. J.; Holland, E. C. Genetically engineered models have advantages over xenografts for preclinical studies. *Cancer Res.* **2006**, *66*, 3355-3358.

(22)Sausville, E. A.; Burger, A. M. Contributions of human tumor xenografts to anticancer drug development. *Cancer Res.* **2006**, *66*, 3351-3354.

(23) Szablowski, J. O.; Raskatov, J. A.; Dervan, P. B. *Unpublished data*.

(24) a) Bao, L.; Matsumura, Y.; Baban, D.; Sun, Y.; Tarin, D. Effects of inoculation site and matrigel on growth and metastasis of human breast-cancer cells. *Br. J. Cancer* **1994**, *70*, 228-232; b) Shuhendler, A. J.; Prasad, P.; Cai, P.; Hui, K. K. W.; Henderson, J. T.; Rauth, A. M.; Wu, X. Y. Matrigel alters the pathophysiology of orthotopic human breast adenocarcinoma xenografts with implications for nanomedicine evaluation. *Nanomed.-Nanotechnol. Biol. Med.* **2013**, *9*, 795-805; c) Fridman, R.; Kibbey, M. C.; Royce, L. S.; Zain, M.; Sweeney, T. M.; Jicha, D. L.; Yannelli, J. R.; Martin, G. R.; Kleinman, H. K. Enhanced Tumor Growth of Both Primary and Established Human and Murine Tumor Cells in Athymic Mice After Coinjection With Matrigel. *J. Natl. Cancer Inst.* **1991**, *83*, 769-774.